



Universiteit
Leiden
The Netherlands

Prediction of biomarker expression on primary pancreatic ductal adenocarcinoma tissues using fine-needle biopsies: paving the way for a patient-tailored molecular imaging approach

Houvast, R.D.; Duijvenvoorde, M. van; Chua, J.; Vankemmelbeke, M.; Durrant, L.G.; Inderson, A.; ... ; Kuppen, P.J.K.

Citation

Houvast, R. D., Duijvenvoorde, M. van, Chua, J., Vankemmelbeke, M., Durrant, L. G., Inderson, A., ... Kuppen, P. J. K. (2023). Prediction of biomarker expression on primary pancreatic ductal adenocarcinoma tissues using fine-needle biopsies: paving the way for a patient-tailored molecular imaging approach. *Molecular Diagnosis & Therapy*, 27, 261-273. doi:10.1007/s40291-022-00635-w

Version: Publisher's Version
License: [Creative Commons CC BY-NC 4.0 license](#)
Downloaded from: <https://hdl.handle.net/1887/3566983>

Note: To cite this publication please use the final published version (if applicable).



Prediction of Biomarker Expression on Primary Pancreatic Ductal Adenocarcinoma Tissues Using Fine-Needle Biopsies: Paving the Way for a Patient-Tailored Molecular Imaging Approach

Ruben D. Houvast¹ · Maurice van Duijvenvoorde¹ · JiaXin Chua² · Mireille Vankemmelbeke² · Lindy G. Durrant^{2,3} · Akin Inderson⁴ · Jeanin E. van Hoof⁴ · J. Sven D. Mieog¹ · Bert A. Bonsing¹ · Cornelis F. M. Sier¹ · A. Stijn L. P. Crobach⁵ · Alexander L. Vahrmeijer¹ · Peter J. K. Kuppen¹

Accepted: 5 December 2022 / Published online: 19 January 2023
© The Author(s) 2023

Abstract

Background Targeted molecular imaging may improve tumor cell identification during diagnosis and resection of pancreatic ductal adenocarcinoma (PDAC). Although many molecular imaging biomarkers are (over)expressed in PDAC, intertumoral heterogeneity of biomarker expression hampers universal tracer administration. Preoperative, patient-specific screening and selection of the most optimal biomarker could therefore improve tumor delineation.

Objective This study evaluated whether fine-needle biopsy (FNB) specimens could be used to preoperatively predict biomarker expression in the corresponding primary PDAC specimen.

Methods Expression of previously identified PDAC biomarkers $\alpha_v\beta_6$, CEACAM5, EGFR, mesothelin, $Le^{a/c/x}$, and sdi- Le^a on FNB and corresponding primary tumor (PT) specimens ($n = 45$) was evaluated using immunohistochemistry and quantified using a semi-automated image analysis workflow.

Results Biomarker expression on FNB and PT tissues showed high concordance (ΔH -score ≤ 50), i.e. was present in 62% of cases for $\alpha_v\beta_6$, 61% for CEACAM5, 85% for EGFR, 69% for mesothelin, 76% for $Le^{a/c/x}$, and 79% for sdi- Le^a , indicating high concordance. Except for $\alpha_v\beta_6$, biomarker expression on FNB tissues was positively correlated with PT expression for all biomarkers. Subgroup analyses showed that neoadjuvant therapy (NAT) had no major and/or significant effect on concordance, expression difference and, except for mesothelin, correlation of biomarker expression between FNB and PT tissues.

Conclusion This study demonstrated that biomarker expression in FNB tissues is predictive for PT expression, irrespective of the application of NAT. These findings thereby provide the foundation for the clinical application of an FNB-based biomarker-screening workflow, eventually facilitating a patient-specific approach of molecular imaging tracer administration in PDAC.

✉ Peter J. K. Kuppen
P.J.K.Kuppen@lumc.nl

¹ Department of Surgery, Leiden University Medical Center, Albinusdreef 2, 2333 ZA Leiden, The Netherlands

² Scancell Limited, University of Nottingham Biodiscovery Institute, University Park, Nottingham NG7 2RD, UK

³ Division of Cancer and Stem Cells, School of Medicine, University of Nottingham Biodiscovery Institute, University Park, Nottingham NG7 2RD, UK

⁴ Department of Gastroenterology and Hepatology, Leiden University Medical Center, Albinusdreef 2, 2333 ZA Leiden, The Netherlands

⁵ Department of Pathology, Leiden University Medical Center, Albinusdreef 2, 2333 ZA Leiden, The Netherlands

Key Points

This is the first study to show that expression of $\alpha_v\beta_6$, CEACAM5, EGFR, mesothelin, $Le^{a/c/x}$, and sdi- Le^a on primary pancreatic ductal adenocarcinoma (PDAC) tissues may be predicted using fine-needle biopsies (FNBs).

The predictive value of FNB expression for primary tumor expression was not negatively influenced by the application of neoadjuvant therapy.

The study facilitates the clinical translation of a personalized molecular imaging approach in PDAC, in which patients can be preoperatively screened for positive biomarker expression, potentially improving both tumor delineation and patient outcomes.

Graphical Abstract

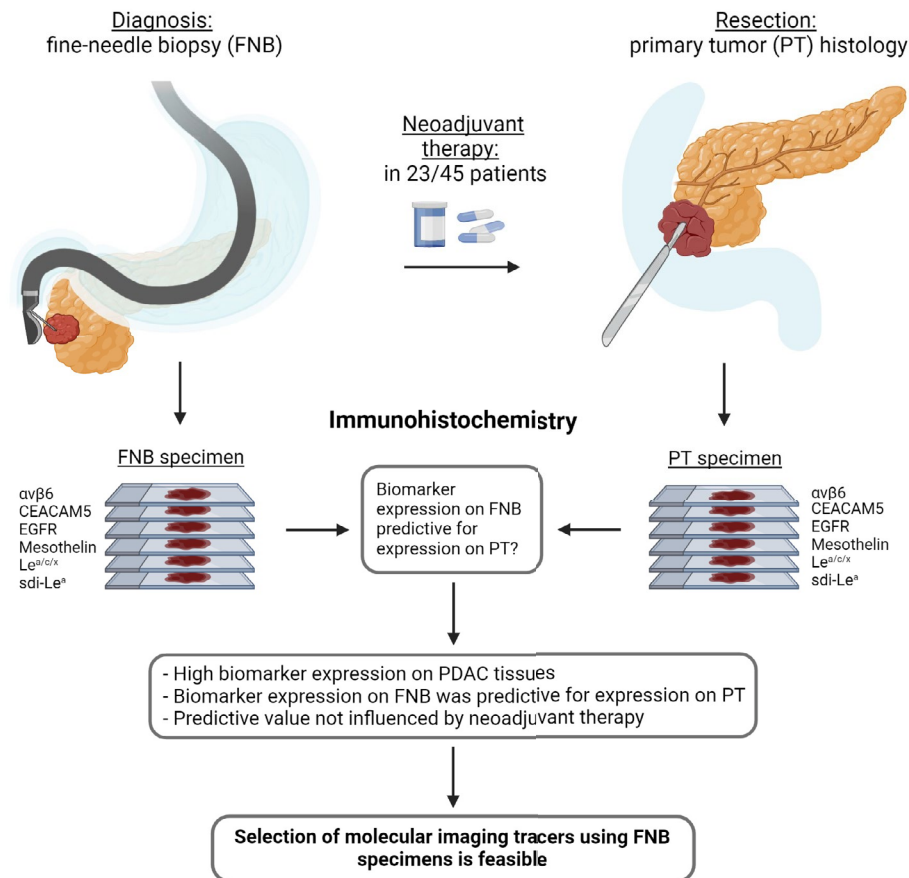
Molecular Diagnosis & Therapy

PEER-REVIEWED
FEATURE

Prediction of Biomarker Expression on Primary Pancreatic Ductal Adenocarcinoma Tissues Using Fine-Needle Biopsies: Paving the Way for a Patient-Tailored Molecular Imaging Approach

Ruben D. Houvast, Maurice van Duijvenvoorde, JiaXin Chua, Mireille Vankemmelbeke, Lindy G. Durrant, Akin Inderson, Jeanin E. van Hooft, J. Sven D. Mieog, Bert A. Bonsing, Cornelis F. M. Sier, A. Stijn L. P. Crobach, Alexander L. Vahrmeijer, Peter J. K. Kuppen

Forty-five pancreatic ductal adenocarcinoma patients



FNB fine-needle biopsy, *PDAC* pancreatic ductal adenocarcinoma, *PT* primary tumor



This graphical abstract represents the opinions of the authors. For a full list of declarations, including funding and author disclosure statements, and copyright information, please see the full text online.

1 Introduction

Pancreatic ductal adenocarcinoma (PDAC) is the most common type of pancreatic cancer ($\pm 90\%$), accounting for approximately 450,000 cases each year worldwide [1]. With a 5-year overall survival rate of merely 2–9%, the malignancy is highly lethal [1, 2]. To date, surgery offers the only curative treatment for PDAC [1–3]. Unfortunately, due to the asymptomatic course of the disease, PDAC is often diagnosed at an advanced stage and therefore only 15–25% of patients qualify for surgery [4]. In addition, positive resection margins are observed in up to 75% of patients who underwent surgery for PDAC, leading to early recurrence and shorter survival [5, 6]. Neoadjuvant therapy (NAT) has been shown to reduce the number of irradical resections and is therefore increasingly applied [7, 8].

Accurate guidance through computed tomography (CT), endoscopic ultrasound (EUS), magnetic resonance imaging (MRI) and/or positron emission tomography (PET) is essential to carefully select and stratify patients for surgery. However, due to the highly infiltrative and discontinuous growth pattern of PDAC, these modalities are not sufficiently able to make a clear distinction between vital tumor cells and benign lesions, such as tumor-associated pancreatitis [9, 10]. Moreover, the application of NAT may induce tissue fibrosis and necrosis, thereby further complicating pre- and intra-operative tumor detection. By providing enhanced contrast between malignant and healthy as well as benign tissues, molecular-targeted imaging agents could provide more reliable visualization of PDAC [11].

Accurate selection of molecular imaging biomarkers remains a key prerequisite for successful tumor delineation. A biomarker is considered suitable for molecular imaging when, among other criteria, it is expressed in a large group of patients within the same tumor type, while expression on surrounding healthy and benign tissues is absent, or at least significantly lower [12]. Previous research by, among others, our group has identified the proteins $\alpha_v\beta_6$, CEACAM5, epidermal growth factor receptor (EGFR), mesothelin, and tumor-associated glycans Lewis^{a/c/x} ($Le^{a/c/x}$) and sialyl-di-Lewis^a (sdi- Le^a) as promising tumor-specific biomarkers for molecular imaging in PDAC [13–17].

Due to the presence of intertumoral heterogeneity and application of NAT, none of these tumor markers is equally expressed in all patients, thereby preventing universal administration of molecular imaging tracers. To address these issues, patients could be preoperatively screened for expression of multiple tumor markers, for instance by using fine-needle biopsies (FNBs). During diagnostic work-up, FNBs are routinely obtained via EUS and may provide histological confirmation of PDAC [18–20]. Moreover, FNB material is increasingly used for molecular and genomic characterization

of PDAC, as well as to generate patient-derived xenografts or organoids, thereby providing opportunities for patient-centered therapeutic selection [21, 22]. Similarly, preoperative evaluation of biomarker expression on FNBs could form a robust and efficient strategy to select the most suitable molecular imaging tracer in a patient-specific manner. However, it remains to be elucidated whether biomarker expression in FNBs corresponds to the expression on the primary tumor (PT). Moreover, very few studies have examined expression of tumor markers in PDAC after NAT [14, 15, 17].

Therefore, this study aimed to evaluate whether preoperative FNB specimens can be used to predict biomarker expression in the corresponding PT specimen. To accomplish this, expression of biomarkers $\alpha_v\beta_6$, CEACAM5, EGFR, mesothelin, $Le^{a/c/x}$ and sdi- Le^a on FNB and PT specimens derived from the same patient was evaluated and compared. Moreover, since FNB specimens are acquired before NAT, the effect of pretreatment on this association between FNB and PT biomarker expression will additionally be studied.

2 Materials and Methods

2.1 Patient and Specimen Selection

Pathology reports of patients who underwent a pancreatic EUS-FNB procedure and resection at the Leiden University Medical Center (LUMC) between 2015 and 2020 were retrospectively reviewed. Representative formalin-fixed paraffin-embedded (FFPE) tissue blocks and hematoxylin and eosin (H&E)-stained slides of the PT and the FNB of each patient were selected, and obtained from the biobank at the LUMC. FNB samples were processed using the cell-block technique [23]. Selection and suitability of patient material included was determined by a hepatopancreaticobiliary pathologist based on H&E slides (ASLPC). One tissue block per FNB or PT tissue was used for each patient. Clinicopathological data were obtained from patients' medical records. Pathological T (pT) and pathological N (pN) stages were defined according to the 8th edition of the American Joint Committee on Cancer/Union for International Cancer Control (AJCC/UICC) TNM staging system for pancreatic cancer. Partial and near-complete pathological response were defined as the presence of $> 5\%$ and $\leq 5\%$ residual tumor tissue, respectively. The study protocol was approved by the Gastroenterology Biobank Review Committee (protocol reference: 2020-16) and the local medical Ethical Review Committee (protocol reference: B20.052). This study was conducted in agreement with the Dutch code of conduct for responsible use of human tissue in medical research. Tissue specimen and clinicopathological data were used anonymized and in compliance with the Declaration of Helsinki (1964).

Table 1 Patient characteristics of the total cohort and subgroups of patients who did and did not receive NAT

Characteristic	Total PDAC [<i>n</i> = 45]	NAT [<i>n</i> = 23]	No NAT [<i>n</i> = 22]	<i>p</i> -value
Age, years [mean (SD)]	64.3 (8.5)	62.7 (7.0)	65.8 (10.0)	0.236
Sex				
Male	18 (40)	9 (39)	9 (41)	0.903
Female	27 (60)	14 (61)	13 (59)	
Tumor differentiation				
Well	4 (9)	1 (4)	3 (14)	^a
Moderate	17 (38)	2 (9)	15 (68)	
Poor	3 (7)	0 (0)	3 (14)	
Missing	21 (47)	20 (87)	1 (4)	
Primary tumor				
pT1	8 (18)	6 (26)	2 (9.0)	0.206
pT2	26 (58)	14 (61)	12 (55)	
pT3	11 (24)	3 (13)	8 (36)	
Regional lymph nodes				
pN0	12 (27)	8 (35)	4 (18)	0.433
pN1	25 (56)	11 (48)	14 (64)	
pN2	8 (18)	4 (17)	4 (18)	
Distant metastases				
M0	43 (96)	22 (96)	21 (96)	0.974
M1	2 (4)	1 (4)	1 (4)	
NAT				
None	22 (49)	NA	22 (100)	–
Gemcitabine/RT	10 (22)	10 (44)	NA	
FOLFIRINOX	13 (29)	13 (57)	NA	
Pathological response				
No response	2 (4)	2 (9)	NA	–
Partial	14 (31)	14 (61)	NA	
Near complete	6 (13)	6 (26)	NA	
Not applicable	22 (49)	0 (0)	22 (100)	
Missing	1 (2)	1 (4)	NA	
Surgery type				
Pancreaticoduodenectomy	33 (73)	18 (78)	15 (68)	0.253
Pancreatic corpus/tail resection	10 (22)	5 (22)	5 (23)	
Total pancreatectomy	2 (5)	0 (0)	2 (9)	
Surgical margin status				
R0	26 (58)	12 (52)	14 (64)	0.436
R1	19 (42)	11 (48)	8 (36)	
Tumor size, mm [mean (SD)]	30 (12)	28 (12)	32 (13)	0.354

Data are expressed as *n* (%) unless otherwise specified

p-values indicate differences in patient characteristics between the no NAT and NAT groups

NA not applicable, NAT neoadjuvant therapy, PDAC pancreatic ductal adenocarcinoma, RT radiotherapy, SD standard deviation

^aCharacteristic is missing for most NAT patients as assessment of tumor differentiation after NAT is not recommended. A statistical comparison of both subgroups is therefore not included

2.2 Immunohistochemistry

Four- μ m-thick tissue sections were cut using a microtome from FFPE tissues and placed on glass slides. Tissue sections were deparaffinized in xylene and rehydrated in degrading

concentrations of ethanol (100%, 50% and 25%), until reaching demineralized water. Subsequently, endogenous peroxidases were blocked using a 0.3% hydrogen peroxide solution. Antigen retrieval was performed depending on the primary antibody as described in Table 1 of the electronic

supplementary material (ESM). After antigen retrieval, slides were rinsed in phosphate-buffered saline (PBS; pH 7.4). Primary antibodies against $\alpha v\beta_6$, CEACAM5, EGFR, mesothelin, $Le^{a/c/x}$ and sdi- Le^a were applied on the tissue and incubated overnight at room temperature in a humid incubator. For information about primary antibodies, see ESM Table 1. After overnight incubation, primary antibodies

were removed by rinsing the slides in PBS, and anti-mouse horseradish peroxidase (HRP) or anti-rabbit HRP secondary antibodies (Envision, Dako, Glostrup, Denmark) were applied for 30 min at room temperature in a humid incubator. Subsequently, secondary antibodies were removed by rinsing the slides in PBS. Antibody binding was visualized using a 3,3-diaminobenzidine tetrahydrochloride solution (DAB, K3468, Agilent Technologies, Inc., Santa Clara, CA, USA) for 10 min at room temperature. Lastly, the slides were counterstained with Mayer's hematoxylin (Klinipath B.V., Olen, Belgium), dehydrated in a dry incubator for 2 h and mounted using pertex (Leica Microsystems, Wetzlar, Germany).

2.3 Semi-Automatic/Digital Image Analysis

Whole slide images of the stained tissue slides were captured using the PANNORAMIC® 250 Flash III DX scanner (3DHISTECH Ltd, Budapest, Hungary). For quantification of DAB staining, QuPath version 0.2.3 open-access software was used [24]. A detailed description of the QuPath workflow used in this study is provided in the ESM. A graphical representation of the used workflow is depicted in ESM Fig. 1. Briefly, random forest object classifiers for PDAC FNB and PT tissues were trained and built for each investigated biomarker separately, yielding a total of 12 object classifiers [25]. Image type settings, color deconvolution stain settings and positive cell detection (DAB staining) parameters were optimized. Object classifiers were trained to specifically recognize and discriminate between tumor cells, stroma cells and red blood cells (RBC), until providing a sensitivity, specificity, negative-predictive value, and positive-predictive value of $\geq 85\%$. Subsequently, the described workflow was scripted, allowing for semi-automated batch processing of the whole cohort ($n = 45$). Tumor regions were annotated on FNB and PT tissues by a pathologist (ASLPCC), whereafter the corresponding script was run. The H-score scoring system was used to quantify per-cell biomarker expression [H-score formula: $1 \times (\% \text{ cells } 1+) + 2 \times (\% \text{ cells } 2+) + 3 \times (\% \text{ cells } 3+)$], in which 1+, 2+ and 3+ were defined as low, medium, and high immunohistochemical staining intensity, respectively. Overall tissue staining with an H-score of ≤ 50 was considered negative, 51–100 as low, 101–200 as moderate, and 201–300 as strong expression of the biomarker. Concordance between fine needle aspiration biopsy (FNAB) and PT biomarker expression was defined as an FNAB versus PT H-score difference of ≤ 50 ($\Delta H\text{-score} \leq 50$).

2.4 Statistical Analysis

IBM SPSS statistics version 25 (IBM Corporation, Armonk, NY, USA) was used for all statistical analyses, and graphs

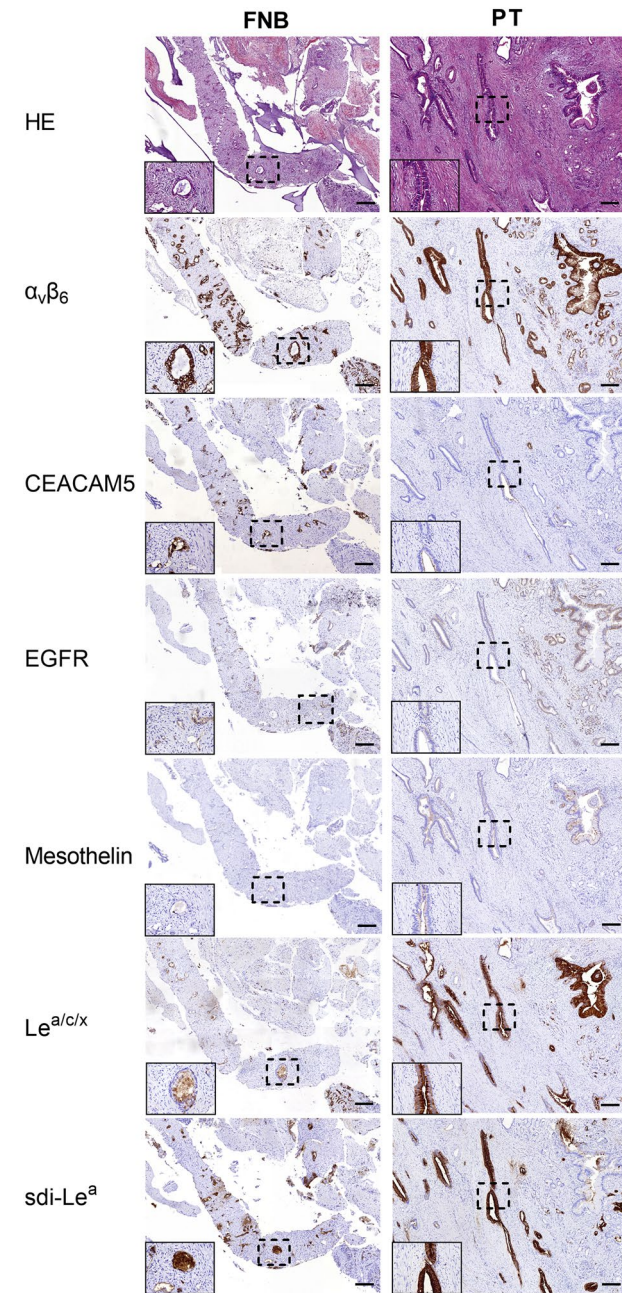


Fig. 1 Images of HE and immunohistochemical staining of $\alpha v\beta_6$, CEACAM5, EGFR, mesothelin, $Le^{a/c/x}$ and sdi- Le^a on FNB and PT tissues derived from one representative patient. Overview images and inserts are taken at 5X and 40X magnification, respectively. Scale bars represent 200 μm . FNB fine-needle biopsy, HE hematoxylin-eosin, PT primary tumor

Table 2 Categorized staining levels of $\alpha_v\beta_6$, CEACAM5, EGFR, mesothelin, $Le^{a/c/x}$ and sdi- Le^a investigated targets in PDAC FNB and PT specimens, separated into cases showing negative (H-score 0–50),

low (H-score 51–100), moderate (H-score 101–200) and strong expression (H-score 201–300)

Biomarker	No. of pairs	Negative		Low		Moderate		Strong	
		FNB	PT	FNB	PT	FNB	PT	FNB	PT
$\alpha_v\beta_6$	42	1 (2)	1 (2)	1 (2)	0 (0)	9 (21)	3 (7)	31 (74)	38 (91)
CEACAM5	41	12 (29)	9 (22)	9 (22)	11 (27)	12 (29)	15 (37)	8 (20)	6 (15)
EGFR	39	0 (0)	4 (10)	7 (18)	6 (15)	30 (77)	24 (62)	2 (5)	5 (13)
Mesothelin	42	26 (62)	22 (52)	7 (17)	10 (24)	9 (21)	8 (19)	0 (0)	2 (5)
$Le^{a/c/x}$	41	4 (10)	6 (15)	2 (5)	6 (15)	21 (51)	17 (42)	14 (34)	12 (29)
sdi- Le^a	43	4 (9)	2 (5)	2 (5)	3 (7)	12 (28)	8 (19)	25 (58)	30 (70)

Data are expressed as n (%)

FNB fine-needle biopsy, PT primary tumor

were created using GraphPad Prism version 8 (GraphPad Software, La Jolla, CA, USA). For categorical data, groups were compared using a Chi-square test. An independent samples t -test was used to compare continuous variables of patient characteristics. Correlation analyses were performed using Spearman correlation. Differences or correlations with a p -value < 0.05 were considered significant.

3 Results

3.1 Patient Characteristics

Forty-five patients diagnosed with PDAC were included in this study, of whom 23 (51%) received NAT and 22 (49%) did not. Ten (43%) NAT patients received gemcitabine/radiotherapy, while 13 (57%) patients received FOLFIRINOX. Characteristics of patients included in the full cohort and within two subgroups (patients who received NAT and patients who did not receive NAT) are shown in Table 1. No significant differences were observed between the two subgroups for all characteristics.

3.2 Object Classifier Training and Validation

Twelve object classifiers were trained and validated. Each of the object classifiers allowed detection of its cell type of interest with sensitivity, specificity, positive predictive value (PPV) and negative predictive value (NPV) of $\geq 85\%$, as shown in ESM Table 2. Examples of QuPath detection images after batch processing analysis in FNB and PT tissues are shown in ESM Fig. 2.

3.3 Biomarker Expression on Fine Needle Biopsy and Primary Tumor Tissues of Pancreatic Ductal Adenocarcinoma

In total, 45 FNB and 45 PT tissues were included in the study and immunohistochemically stained for $\alpha_v\beta_6$, CEACAM5, EGFR, mesothelin, $Le^{a/c/x}$ and sdi- Le^a expression, followed by staining quantification using the described semi-automated imaging analysis workflow. Sequential images of staining of FNB and PT tissues derived from one representative patient are shown in Fig. 1.

All biomarkers showed a membranous staining pattern on tumor cells in both FNB and PT tissues, with CEACAM5 showing generally more staining on the luminal side of cells. $\alpha_v\beta_6$ was homogeneously expressed throughout the positive tumors, whereas $Le^{a/c/x}$ and sdi- Le^a showed a slightly more heterogenous staining pattern. Membranous staining of CEACAM5, EGFR and mesothelin on PDAC cells was considerably more heterogeneous compared with the other biomarkers (Fig. 1).

In the FNB specimen, positive biomarker expression (H-score > 51) was observed in 41/42 (98%) for $\alpha_v\beta_6$, 29/41 (71%) for CEACAM5, 39/39 (100%) for EGFR, 16/42 (38%) for mesothelin, 37/41 (90%) for $Le^{a/c/x}$ and 39/43 (91%) for sdi- Le^a . In the PT specimen, positive biomarker expression was observed in 41/42 (98%) for $\alpha_v\beta_6$, 32/41 (78%) for CEACAM5, 35/39 (90%) for EGFR, 20/42 (48%) for mesothelin, 35/41 (85%) for $Le^{a/c/x}$ and 41/43 (95%) for sdi- Le^a . Categorized biomarker staining levels for FNB and PT tissues separately are shown in Table 2. Moderate or strong $\alpha_v\beta_6$, $Le^{a/c/x}$ and sdi- Le^a staining was observed in most FNB and PT tissues, whereas EGFR was moderately stained in the majority of cases. CEACAM5 and mesothelin staining was generally weaker compared with the other biomarkers.

Table 3 Concordance rates biomarker expression on FNB and PT tissues for the full cohort as well as the NAT and no NAT subgroups, along with the number of FNB and PT pairs

Biomarker	Full cohort concordance		Subgroup concordance		
	No. of pairs	Patients Δ H-score ≤ 50 [n (%)]	No. of pairs	Treatment	Patients Δ H-score ≤ 50 [n (%)]
$\alpha_v\beta_6$	42	26 (62)	22	NAT	14 (64)
			20	No NAT	12 (60)
CEACAM5	41	25 (61)	21	NAT	15 (71)
			20	No NAT	14 (70)
EGFR	39	33 (85)	18	NAT	15 (83)
			21	No NAT	18 (86)
Mesothelin	42	29 (69)	22	NAT	17 (77)
			20	No NAT	12 (60)
Le ^{a/c/x}	41	31 (76)	22	NAT	18 (82)
			19	No NAT	13 (68)
sdi-Le ^a	43	34 (79)	23	NAT	16 (70)
			20	No NAT	18 (90)

Concordance of biomarker expression was present when the H-score difference between FNB and PT tissues (Δ H-score) was ≤ 50

NAT neoadjuvant therapy, FNB fine-needle biopsy, PT primary tumor

3.4 Concordance Between Biomarker Expression on PDAC FNB and PT Tissues

To assess the concordance between FNB and PT biomarker expression, differences between H-scores on FNB and PT tissue were calculated. Concordance was considered to be present when the difference between FNB and PT H-score was ≤ 50 . Concordance rates of all biomarkers are shown in Table 3. For the full cohort, concordance rates were 62% for $\alpha_v\beta_6$, 61% for CEACAM5, 85% for EGFR, 69% for mesothelin, 76% for Le^{a/c/x} and 79% for sdi-Le^a, indicating high concordance between biomarker expression on FNB and PT tissues. Next, to study the effect of NAT on concordance between FNB and PT biomarker expression, patients who did and did not receive NAT were divided into two subgroups. In subgroup analyses, medium to high concordance rates between dichotomized IHC staining were observed for patients who received NAT (range 64–83%) and patients who did not (range 60–90%), suggesting that NAT does not substantially affect concordance between positive or negative FNB and PT biomarker expression (Table 3).

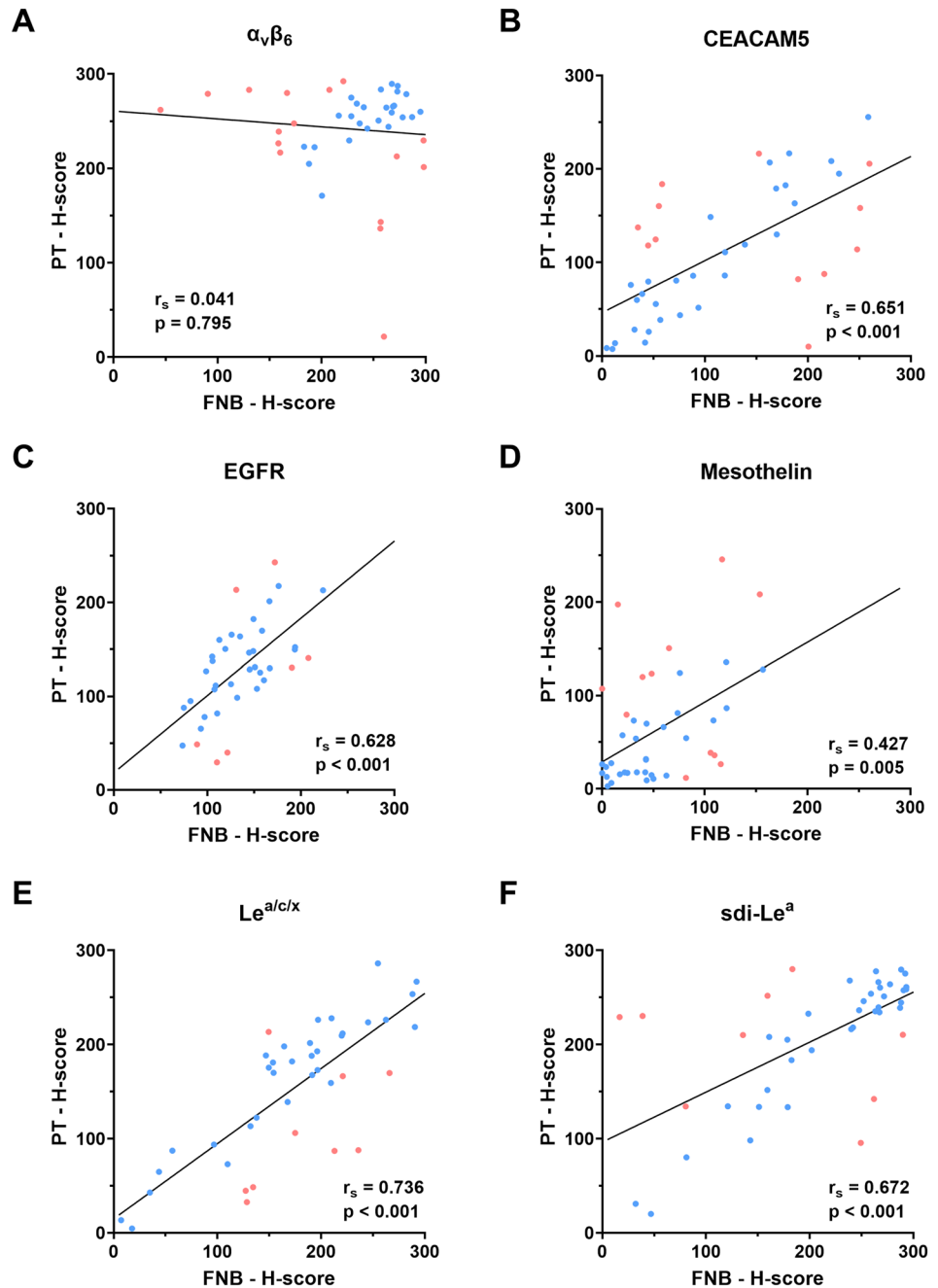
3.5 Correlation between Biomarker Expression on PDAC FNB and PT Tissues

To study the predictive value of biomarker expression on FNB tissues for PT expression, the relationship of biomarker

expression levels between FNB and PT specimens was investigated. For the full cohort, H-score scatterplots showing biomarker expression on FNB and PT tissues are shown in Fig. 2a–f. Moreover, Spearman's rank correlation coefficients indicating the linear association between the FNB and PT biomarker expression are shown in Table 4 as well as in Fig. 2a–f. H-scores on FNB tissues were positively correlated with H-scores on PT tissues for CEACAM5, EGFR, mesothelin, sdi-Le^a and Le^{a/c/x}, suggesting that biomarker expression on FNB tissues is predictive for expression level in PT tissues. Correlation coefficients indicated a moderate–strong linear relationship between FNB and PT expression. However, for $\alpha_v\beta_6$, no correlation between H-score on FNB and PT tissues was found ($r_s = 0.041$, $p = 0.795$).

Next, subgroup analyses were performed to study the effect of NAT on the predictive value of biomarker expression on FNB tissues for PT biomarker expression. As shown in Fig. 3a–l and Table 5, H-scores of CEACAM5, EGFR, sdi-Le^a and Le^{a/c/x} expression on FNB were positively correlated with H-scores on PT tissues in both NAT and no NAT patients, suggesting that biomarker expression is predictive for PT expression regardless of application of NAT. However, for $\alpha_v\beta_6$ and mesothelin, biomarker expression on FNB tissues was not predictive for PT expression regardless of application of NAT or in the no NAT subgroup, respectively.

Fig. 2 H-score scatterplots showing the relationship between immunohistochemical staining of **a** $\alpha_v\beta_6$, **b** CEACAM5, **c** EGFR, **d** mesothelin, **e** $Le^{a/c/x}$ and **f** sdi- Le^a on FNB (x-axis) and PT (y-axis) tissues. Blue dots represent an H-score difference between FNB and PT staining of ≤ 50 , whereas the red dots represent a difference of > 51 , thereby indicating an outlier. Spearman's rank correlation coefficients (r_s) with their corresponding p -values are shown in each graph. *FNB* fine-needle biopsy, *PT* primary tumor



4 Discussion

Tumor-targeted molecular imaging could play a crucial role in solving current challenges during diagnosis, monitoring and resection of PDAC by providing high-contrast delineation of malignant tissues [11, 26]. Patient-specific screening and selection of molecular imaging biomarkers using FNB tissues may improve PDAC delineation and prevent unnecessary tracer administration.

Our study shows that $\alpha_v\beta_6$, CEACAM5, EGFR, mesothelin, $Le^{a/c/x}$ and sdi- Le^a are highly expressed in FNB and PT tissues of PDAC. The results suggest that there is a high level of association in expression between FNB and PT tissues of PDAC for the biomarkers evaluated herein. Although no correlation was observed for $\alpha_v\beta_6$, concordance rate was the highest among the investigated biomarkers. This suggests that $\alpha_v\beta_6$ expression is similar between FNB and PT, and the biomarker was expressed in an homogenous manner, i.e. strongly in most tissues. Moreover, when discriminating between patients who received NAT and patients who

Table 4 Correlation scores between biomarker expression on FNB and PT PDAC tissues

Biomarker	No. of pairs	Correlation	
		r_s	p -value
$\alpha_v\beta_6$	42	0.041	0.795
CEACAM5	41	0.651	< 0.001
EGFR	39	0.628	< 0.001
Mesothelin	42	0.427	0.005
Le ^{al/c/x}	41	0.736	< 0.001
sdi-Le ^a	43	0.672	< 0.001

Spearman's rank correlation coefficients (r_s) along with their corresponding p -values are shown

FNB fine-needle biopsy, PT primary tumor, PDAC pancreatic ductal adenocarcinoma

received no NAT, no substantial differences between concordance rates and correlations, except for mesothelin, were observed, suggesting that NAT does not affect the expression level of the biomarkers investigated and therefore also not the predictive value of biomarker expression on FNB versus PT tissues. Our study therefore demonstrated the feasibility of a molecular imaging biomarker screening workflow for PDAC in a clinically relevant setting.

The current findings are largely in line with previous studies that showed high expression of $\alpha_v\beta_6$, CEACAM5, EGFR, mesothelin, Le^{al/c/x} and sdi-Le^a in PDAC tissues [13–15, 17]. Interestingly, our study found positive mesothelin expression in 48% of PT tissues, while most studies report positive mesothelin expression in 80–85% of PDAC tissues [15, 27, 28]. This discrepancy could have been caused by, among others, the use of different antibody clones directed against mesothelin, a lack of staining reproducibility between laboratories, or the use of manual scoring methods in other studies, which may not be sufficiently reproducible [29–31]. Biopsy specimens have the potential to aid in proper treatment selection, as was previously shown for rectum, lung, breast and gastric cancer [32–36]. In each of these studies, high levels of concordance between biomarker expression on biopsy and PT tissues was observed. Although PDAC FNB specimens are already used in research into PDAC diagnosis [37–39], the association between FNB and PT biomarker expression has, to the best of our knowledge, not yet been investigated for PDAC.

The lack of reproducibility of manual scoring was compensated in our study through the use of QuPath, which could provide superior cell detection efficacy, leading to more accurate and reproducible H-scores as opposed to manual scoring [24, 31]. However, the QuPath workflow we used herein was more time-consuming compared with manual scoring. We therefore believe that for this study,

the advantages outweighed the disadvantages as the workflow allowed us to obtain highly accurate and reproducible results.

Although moderate to strong correlation coefficients between FNB and PT tissues were observed for expression levels of most biomarkers, along with high concordance, several H-score outliers were present. A possible explanation may be that, considering the average time of 100 days between the FNB and surgical procedure (data not shown), biomarker expression changed over time. PDAC is a highly progressive disease and distinct (epi)genetic events or remodeling could lead to a certain extent of polyclonality [17, 18]. Different subclones of tumor cells could (over) express distinct proteins and, over time, this could result in intra-tumoral heterogeneity and, subsequently, varying expression patterns. Second, a biopsy is merely a small fragment of the entire PT specimen. Considering intra-tumoral heterogeneity, it could very well be possible that a biopsy sample contains an area of the PT that does not express the biomarker of interest, while other parts of the tumor do express the biomarker [17]. Of note, and in line with previous research, five of six biomarkers evaluated herein showed considerable heterogeneity, further substantiating this hypothesis [13–17, 27]. Lastly, FNB cell blocks and FFPE tissues are fixed and processed differently, which can influence the level of IHC staining [40]. However, our study shows that in most cases, biomarker expression on FNB tissues shows considerable predictivity for expression on PT tissues, indicating that biopsy specimens provide a representative sample of PT tissues.

Due to their low abundance in surrounding tissues, and also high expression in lymph node metastases, the biomarkers evaluated herein are promising targets for both diagnostic and intraoperative imaging of PDAC. Regarding the former, several studies recently reported the phase I/II evaluation of targeted PET tracers directed against mesothelin and $\alpha_v\beta_6$ and showed their safety and feasibility for PDAC visualization [41–43]. With regard to the latter, (early-phase) clinical trials have particularly focused on NIRF tracers targeting EGFR and CEA [44–48]. NIRF imaging using the anti-EGFR tracers panitumumab-IRDye800CW and cetuximab-IRDye800CW, and anti-CEA tracer SGM-101, allowed clear delineation of primary PDAC lesions, as well as lymph node and distant metastases intraoperatively [44–48]. Within the preclinical arena, the anti- $\alpha_v\beta_6$ tracers R01-MG-IRDye800CW and anti-Le^{al/c/x} CH88.2-IRDye800CW have enabled clear localization and delineation of human PDAC xenografts in mice, thereby strengthening their clinical potential for real-time intraoperative NIRF imaging of PDAC [16, 49]. Considering the (pre)clinical availability of molecular tracers directed against these biomarkers, the workflow we evaluate and discuss in this study may be instantaneously translated towards a clinical setting, where

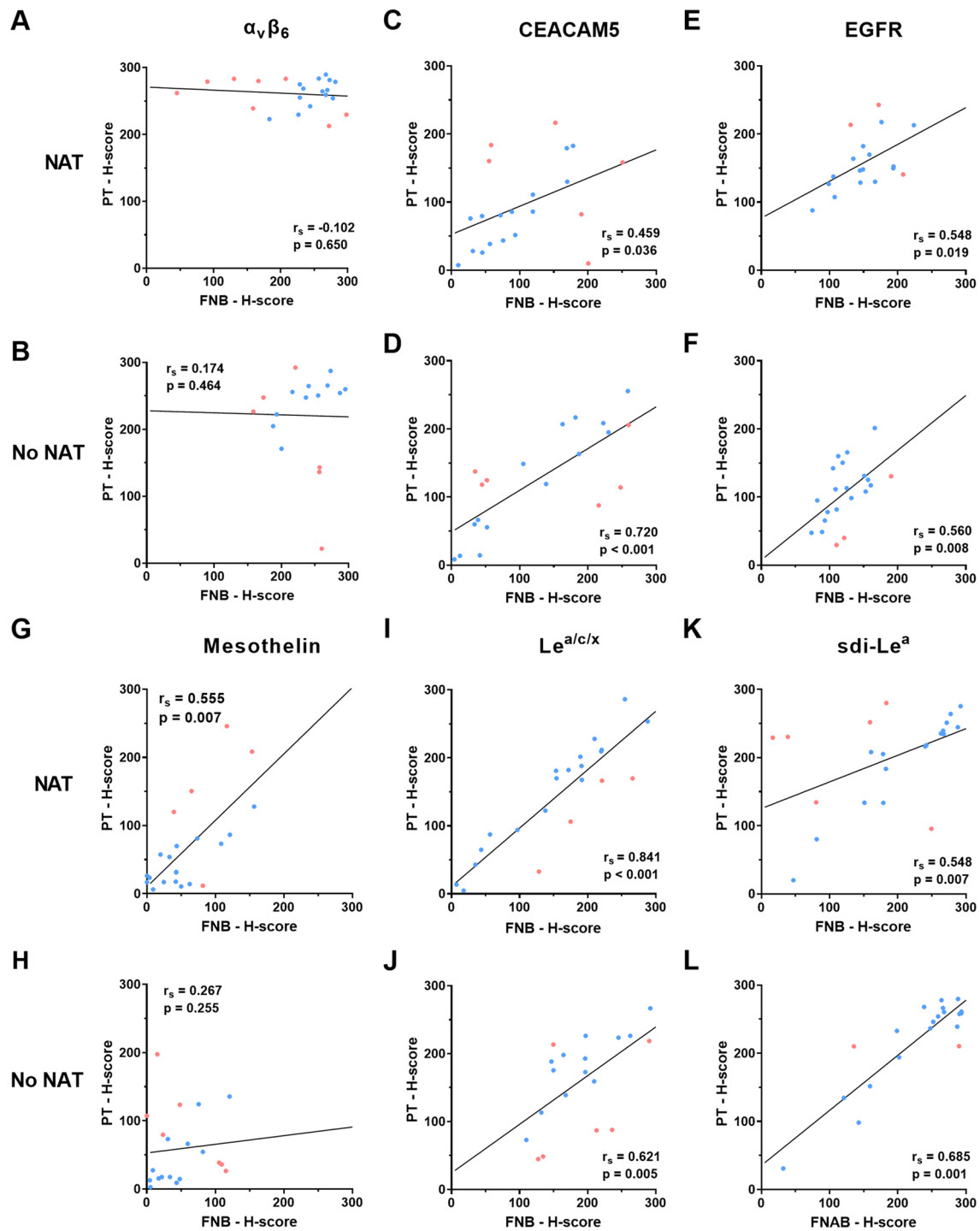


Fig. 3 H-score scatterplots showing the relationship between immunohistochemical staining of **a, b** $\alpha_v\beta_6$, **c, d** CEACAM5, **e, f** EGFR, **g, h** mesothelin, **i, j** Le^{a/c/x} and **k, l** sdi-Le^a on FNB (x-axis) and PT (y-axis) tissues for NAT and no NAT patients separately. Blue dots represent an H-score difference between FNB and PT staining of

≤ 50 , whereas the red dots represent a difference of > 51 , thereby indicating an outlier. Spearman's rank correlation coefficients (r_s) with their corresponding p -values are shown in each graph. *FNB* fine-needle biopsy, *NAT* neoadjuvant therapy, *PT* primary tumor

patients with positive biomarker expression in FNB can be selected for patient-specific tracer administration.

This study has some limitations. First, the present study cohort was relatively small for exact estimation of biomarker

expression in PT tissues. Therefore, evaluation of the relationship between FNB and PT expression on a larger cohort could strengthen the findings of this study. Second, due to the limited number of patients available, the NAT subgroup

Table 5 Correlation scores between biomarker expression on FNB and PT PDAC tissues, subdivided into patients who received NAT and patients who did not

Biomarker		No. of pairs	Correlation	
			r_s	p -value
$\alpha_v\beta_6$	NAT	22	-0.102	0.650
	No NAT	20	0.174	0.464
CEACAM5	NAT	21	0.459	0.036
	No NAT	20	0.720	< 0.001
EGFR	NAT	18	0.548	0.019
	No NAT	21	0.560	0.008
Mesothelin	NAT	22	0.555	0.007
	No NAT	20	0.267	0.255
Le ^{a/c/x}	NAT	22	0.841	< 0.001
	No NAT	19	0.621	0.005
sdi-Le ^a	NAT	23	0.548	0.007
	No NAT	20	0.685	0.001

Spearman's rank correlation coefficients (r_s) along with their corresponding p -values are shown

NAT neoadjuvant therapy, FNB fine-needle biopsy, PT primary tumor, PDAC pancreatic ductal adenocarcinoma

was small, which allowed no separate evaluation of the effect of gemcitabine/radiotherapy or FOLFIRINOX. Third, due to staining artefacts, the number of pairs available for analysis differed and did not overlap precisely for all biomarkers.

Future research could focus on the expansion of the workflow to other tumor types for which biopsies are obtained, such as breast, (colo)rectal and gastric cancer, and additionally to other tumor biomarkers of interest. The workflow evaluated herein can conveniently be integrated within standard pathological work-up, as IHC stainings on FNB tissues for markers such as Ki-67, p53 and SMAD4 are regularly performed to guide histological diagnosis [50–52]. Taken further, this method of biomarker screening can also be applied in the therapeutic arena, where PDAC patients eligible for targeted therapy can be screened for biomarker expression (53). Overall, this study provides the foundation for clinical translation of a patient-specific, FNB-based molecular imaging biomarker selection workflow that may improve PDAC diagnosis, delineation, and, ultimately, patient outcomes.

5 Conclusion

Our findings show that biomarker expression on FNB is considerably predictive for biomarker expression on corresponding PT tissue, irrespective of the application of NAT.

This study thereby provides the foundation for the clinical application of an FNB-based biomarker-screening workflow, eventually facilitating a personalized approach of molecular imaging tracer administration in PDAC.

Supplementary Information The online version contains supplementary material available at <https://doi.org/10.1007/s40291-022-00635-w>.

Acknowledgments The authors thank Ronald van Vlierberghe and Shadhvi Bhariosingh for their help with immunohistochemistry and tissue slide scanning.

Data Availability The data presented in this study are available upon reasonable request from the corresponding author.

Declarations

Funding No external funding was obtained for this study.

Conflicts of interest Lindy G. Durrant is CEO and CSO of Scancell Ltd and has an ownership interest in the company. JiaXin Chua and Mireille Vankemmelbeke are employed by Scancell Ltd. Ruben D. Houvast, Maurice van Duijvenvoorde, Akin Inderson, Jeanin E. van Hooft, J. Sven D. Mieog, Bert A. Bonsing, Cornelis F.M. Sier, A. Stijn L.P. Crobach, Alexander L. Vahrmeijer and Peter J.K. Kuppen declare no conflicts of interest.

Ethics approval The study protocol was approved by the Gastroenterology Biobank Review Committee (protocol reference: 2020-16) and local Medical Ethical Review Committee (protocol reference: B20.052). The research was conducted in accordance with the Dutch code of conduct for responsible use of human tissue in medical research. Tissue specimens and clinicopathological data were used anonymized and in compliance with the Declaration of Helsinki (1964).

Consent to participate The need for informed consent was waived by the local Medical Ethical Review Committee.

Consent for publication Not applicable.

Availability of data, material and code The data presented in this study are available upon reasonable request from the corresponding author.

Author contributions RDH and MvD were responsible for conceptualization, methodology, formal analysis and visualization. RDH wrote the original draft of the manuscript. All remaining authors contributed to reviewing and editing of the manuscript. PJKK was responsible for supervision. All authors read and approved the final version of the manuscript.

Open Access This article is licensed under a Creative Commons Attribution-NonCommercial 4.0 International License, which permits any non-commercial use, sharing, adaptation, distribution and reproduction in any medium or format, as long as you give appropriate credit to the original author(s) and the source, provide a link to the Creative Commons licence, and indicate if changes were made. The images or other third party material in this article are included in the article's Creative Commons licence, unless indicated otherwise in a credit line to the material. If material is not included in the article's Creative Commons licence and your intended use is not permitted by statutory regulation or exceeds the permitted use, you will need to obtain permission

directly from the copyright holder. To view a copy of this licence, visit <http://creativecommons.org/licenses/by-nc/4.0/>.

References

- McGuigan A, Kelly P, Turkington RC, Jones C, Coleman HG, McCain RS. Pancreatic cancer: a review of clinical diagnosis, epidemiology, treatment and outcomes. *World J Gastroenterol*. 2018;24(43):4846–61.
- Latenstein AEJ, van der Geest LGM, Bonsing BA, Groot Koerkamp B, Haj Mohammad N, de Hingh I, et al. Nationwide trends in incidence, treatment and survival of pancreatic ductal adenocarcinoma. *Eur J Cancer*. 2020;125:83–93.
- Stathis A, Moore MJ. Advanced pancreatic carcinoma: current treatment and future challenges. *Nat Rev Clin Oncol*. 2010;7(3):163–72.
- Barugola G, Partelli S, Marcucci S, Sartori N, Capelli P, Bassi C, et al. Resectable pancreatic cancer: who really benefits from resection? *Ann Surg Oncol*. 2009;16(12):3316–22.
- Tummers WS, Groen JV, Sibinga Mulder BG, Farina-Sarasqueta A, Morreau J, Putter H, et al. Impact of resection margin status on recurrence and survival in pancreatic cancer surgery. *Br J Surg*. 2019;106(8):1055–65.
- Verbeke CS. Resection margins in pancreatic cancer. *Surg Clin North Am*. 2013;93(3):647–62.
- Versteijne E, Suker M, Groothuis K, Akkermans-Vogelaar JM, Besselink MG, Bonsing BA, et al. Preoperative chemoradiotherapy versus immediate surgery for resectable and borderline resectable pancreatic cancer: results of the dutch randomized phase III PREOPANC trial. *J Clin Oncol*. 2020;38(16):1763–73.
- Janssen QP, van Dam JL, Bonsing BA, Bos H, Bosscha KP, Coene P, et al. Total neoadjuvant FOLFIRINOX versus neoadjuvant gemcitabine-based chemoradiotherapy and adjuvant gemcitabine for resectable and borderline resectable pancreatic cancer (PREOPANC-2 trial): study protocol for a nationwide multicenter randomized controlled trial. *BMC Cancer*. 2021;21(1):300.
- Ferrone CR, Marchegiani G, Hong TS, Ryan DP, Deshpande V, McDonnell EI, et al. Radiological and surgical implications of neoadjuvant treatment with FOLFIRINOX for locally advanced and borderline resectable pancreatic cancer. *Ann Surg*. 2015;261(1):12–7.
- González-Gómez R, Pazo-Cid RA, Sarría L, Morcillo M, Schuhmacher AJ. Diagnosis of pancreatic ductal adenocarcinoma by immuno-positron emission tomography. *J Clin Med*. 2021;10(6):1151.
- Tummers WS, Willmann JK, Bonsing BA, Vahrmeijer AL, Gambhir SS, Swijnenburg RJ. Advances in diagnostic and intraoperative molecular imaging of pancreatic cancer. *Pancreas*. 2018;47(6):675–89.
- Hernot S, van Manen L, Debie P, Mieog JSD, Vahrmeijer AL. Latest developments in molecular tracers for fluorescence image-guided cancer surgery. *Lancet Oncol*. 2019;20(7):e354–67.
- de Geus SW, Boogerd LS, Swijnenburg RJ, Mieog JS, Tummers WS, Prevo HA, et al. Selecting tumor-specific molecular targets in pancreatic adenocarcinoma: paving the way for image-guided pancreatic surgery. *Mol Imaging Biol*. 2016;18(6):807–19.
- Tummers WS, Farina-Sarasqueta A, Boonstra MC, Prevo HA, Sier CF, Mieog JS, et al. Selection of optimal molecular targets for tumor-specific imaging in pancreatic ductal adenocarcinoma. *Oncotarget*. 2017;8(34):56816–28.
- Vuijk FA, de Muynck L, Franken LC, Busch OR, Wilmink JW, Besselink MG, et al. Molecular targets for diagnostic and intraoperative imaging of pancreatic ductal adenocarcinoma after neoadjuvant FOLFIRINOX treatment. *Sci Rep*. 2020;10(1):16211.
- Houvast RD, Baart VM, Bhairosingh SS, Cordfunke RA, Chua JX, Vankemmelbeke M, et al. Glycan-Based Near-infrared Fluorescent (NIRF) Imaging of Gastrointestinal Tumors: a Pre-clinical Proof-of-Concept In Vivo Study. *Mol Imaging Biol*. 2020;22(6):1511–22.
- Houvast RD, Thijse K, Groen JV, Chua J, Vankemmelbeke M, Durrant LG, et al. An immunohistochemical evaluation of tumor-associated glycans and mucins as targets for molecular imaging of pancreatic ductal adenocarcinoma. *Cancers (Basel)*. 2021;13(22):5777.
- Kalogeraki A, Papadakis GZ, Tamiolakis D, Karvela-Kalogeraki I, Karvelas-Kalogerakis M, Segredakis J, et al. EUS-fine-needle aspiration biopsy (FNAB) in the diagnosis of pancreatic adenocarcinoma: a review. *Rom J Intern Med*. 2016;54(1):24–30.
- Luu TT. Review of immunohistochemistry biomarkers in pancreatic cancer diagnosis. *Front Oncol*. 2021;11: 799025.
- Bang JY, Hebert-Magee S, Navaneethan U, Hasan MK, Hawes R, Varadarajulu S. EUS-guided fine needle biopsy of pancreatic masses can yield true histology. *Gut*. 2018;67(12):2081–4.
- Archibugi L, Testoni SGG, Redegalli M, Petrone MC, Reni M, Falconi M, et al. New era for pancreatic endoscopic ultrasound: From imaging to molecular pathology of pancreatic cancer. *World J Gastrointest Oncol*. 2019;11(11):933–45.
- Tanaka H, Matsusaki S. The utility of endoscopic-ultrasonography-guided tissue acquisition for solid pancreatic lesions. *Diagnostics (Basel)*. 2022;12(3):753.
- Ieni A, Barresi V, Todaro P, Caruso RA, Tuccari G. Cell-block procedure in endoscopic ultrasound-guided-fine-needle-aspiration of gastrointestinal solid neoplastic lesions. *World J Gastrointest Endosc*. 2015;7(11):1014–22.
- Bankhead P, Loughrey MB, Fernández JA, Dombrowski Y, McArt DG, Dunne PD, et al. QuPath: open source software for digital pathology image analysis. *Sci Rep*. 2017;7(1):16878.
- Breiman L. Random forests. *Mach Learn*. 2001;45(1):5–32.
- Vahrmeijer AL, Hutteman M, van der Vorst JR, van de Velde CJ, Frangioni JV. Image-guided cancer surgery using near-infrared fluorescence. *Nat Rev Clin Oncol*. 2013;10(9):507–18.
- Le K, Wang J, Zhang T, Guo Y, Chang H, Wang S, et al. Overexpression of mesothelin in pancreatic ductal adenocarcinoma (PDAC). *Int J Med Sci*. 2020;17(4):422–7.
- Montemagno C, Cassim S, Pouyssegur J, Broisat A, Pagès G. From malignant progression to therapeutic targeting: current insights of mesothelin in pancreatic ductal adenocarcinoma. *Int J Mol Sci*. 2020;21(11):4067.
- Adams EJ, Green JA, Clark AH, Youngson JH. Comparison of different scoring systems for immunohistochemical staining. *J Clin Pathol*. 1999;52(1):75–7.
- Loughrey MB, Bankhead P, Coleman HG, Hagan RS, Craig S, McCorry AMB, et al. Validation of the systematic scoring of immunohistochemically stained tumour tissue microarrays using QuPath digital image analysis. *Histopathology*. 2018;73(2):327–38.
- Bankhead P, Fernández JA, McArt DG, Boyle DP, Li G, Loughrey MB, et al. Integrated tumor identification and automated scoring minimizes pathologist involvement and provides new insights to key biomarkers in breast cancer. *Lab Invest*. 2018;98(1):15–26.
- Boogerd LS, van der Valk MJ, Boonstra MC, Prevo HA, Hilling DE, van de Velde CJ, et al. Biomarker expression in rectal cancer tissue before and after neoadjuvant therapy. *Oncotargets Ther*. 2018;11:1655–64.
- Okimoto T, Tsubata Y, Sutani A, Fuchita H, Koba N, Hotta T, et al. Immunohistochemical comparison of biomarker expression

- in biopsy and surgical specimens of non-small cell lung cancer. *Anticancer Res.* 2014;34(6):2755–61.
34. Robertson S, Rönnlund C, de Boniface J, Hartman J. Re-testing of predictive biomarkers on surgical breast cancer specimens is clinically relevant. *Breast Cancer Res Treat.* 2019;174(3):795–805.
 35. Taillade L, Penault-Llorca F, Boulet T, Fouret P, Michiels S, Taranchon E, et al. Immunohistochemical expression of biomarkers: a comparative study between diagnostic bronchial biopsies and surgical specimens of non-small-cell lung cancer. *Ann Oncol.* 2007;18(6):1043–50.
 36. Wang T, Hsieh ET, Henry P, Hanna W, Streutker CJ, Grin A. Matched biopsy and resection specimens of gastric and gastroesophageal adenocarcinoma show high concordance in HER2 status. *Hum Pathol.* 2014;45(5):970–5.
 37. Agarwal B, Ludwig OJ, Collins BT, Cortese C. Immunostaining as an adjunct to cytology for diagnosis of pancreatic adenocarcinoma. *Clin Gastroenterol Hepatol.* 2008;6(12):1425–31.
 38. Zapata M, Cohen C, Siddiqui MT. Immunohistochemical expression of SMAD4, CK19, and CA19-9 in fine needle aspiration samples of pancreatic adenocarcinoma: utility and potential role. *Cytojournal.* 2007;4:13.
 39. Nguyen NQ, Ruzskiewicz A, Chang D, Bambrick J, Biankin AV. Biomarker assessment from EUS-guided biopsy to predict outcomes and treatment in pancreatic cancer. *J Clin Oncol.* 2014;32(3 Suppl):182.
 40. Shidham VB, Layfield LJ. Cell-blocks and immunohistochemistry. *Cytojournal.* 2021;18:2.
 41. Lamberts LE, Koch M, de Jong JS, Adams ALL, Glatz J, Kranendonk MEG, et al. Tumor-specific uptake of fluorescent bevacizumab-IRDye800CW microdosing in patients with primary breast cancer: a phase I feasibility study. *Clin Cancer Res.* 2017;23(11):2730–41.
 42. Kimura RH, Wang L, Shen B, Huo L, Tummers W, Filipp FV, et al. Evaluation of integrin $\alpha v \beta 6$ cystine knot PET tracers to detect cancer and idiopathic pulmonary fibrosis. *Nat Commun.* 2019;10(1):4673.
 43. Nakamoto R, Ferri V, Duan H, Hatami N, Goel M, Rosenberg J, et al. Pilot-phase PET/CT study targeting integrin $\alpha(v)\beta(6)$ in pancreatic cancer patients using the cystine-knot peptide-based (18)F-FP-R(0)1-MG-F2. *Eur J Nucl Med Mol Imaging.* 2022;50(1):184–93.
 44. Hoogstins CES, Boogerd LSF, Sibinga Mulder BG, Mieog JSD, Swijnenburg RJ, van de Velde CJH, et al. Image-guided surgery in patients with pancreatic cancer: first results of a clinical trial using SGM-101, a novel carcinoembryonic antigen-targeting, a near-infrared fluorescent agent. *Ann Surg Oncol.* 2018;25(11):3350–7.
 45. Tummers WS, Miller SE, Teraphongphom NT, Gomez A, Steinberg I, Huland DM, et al. Intraoperative pancreatic cancer detection using tumor-specific multimodality molecular imaging. *Ann Surg Oncol.* 2018;25(7):1880–8.
 46. Tummers WS, Miller SE, Teraphongphom NT, van den Berg NS, Hasan A, Longacre TA, et al. Detection of visually occult metastatic lymph nodes using molecularly targeted fluorescent imaging during surgical resection of pancreatic cancer. *HPB (Oxford).* 2019;21(7):883–90.
 47. Lu G, van den Berg NS, Martin BA, Nishio N, Hart ZP, van Keulen S, et al. Tumour-specific fluorescence-guided surgery for pancreatic cancer using panitumumab-IRDye800CW: a phase 1 single-centre, open-label, single-arm, dose-escalation study. *Lancet Gastroenterol Hepatol.* 2020;5(8):753–64.
 48. Boogerd LSF, Hoogstins CES, Schaap DP, Kusters M, Handgraaf HJM, van der Valk MJM, et al. Safety and effectiveness of SGM-101, a fluorescent antibody targeting carcinoembryonic antigen, for intraoperative detection of colorectal cancer: a dose-escalation pilot study. *Lancet Gastroenterol Hepatol.* 2018;3(3):181–91.
 49. Tummers WS, Kimura RH, Abou-Elkacem L, Beinat C, Vahrmeijer AL, Swijnenburg RJ, et al. Development and preclinical validation of a cysteine knottin peptide targeting integrin $\alpha v \beta 6$ for near-infrared fluorescent-guided surgery in pancreatic cancer. *Clin Cancer Res.* 2018;24(7):1667–76.
 50. Jahng AW, Reicher S, Chung D, Varela D, Chhablani R, Dev A, et al. Staining for p53 and Ki-67 increases the sensitivity of EUS-FNA to detect pancreatic malignancy. *World J Gastrointest Endosc.* 2010;2(11):362–8.
 51. Fabbri C, Gibiino G, Fornelli A, Cennamo V, Grifoni D, Visani M, et al. Team work and cytopathology molecular diagnosis of solid pancreatic lesions. *Dig Endosc.* 2017;29(6):657–66.
 52. Ren B, Liu X, Suriawinata AA. Pancreatic ductal adenocarcinoma and its precursor lesions: histopathology, cytopathology, and molecular pathology. *Am J Pathol.* 2019;189(1):9–21.
 53. Lundy J, Harris M, Zalcborg J, Zimet A, Goldstein D, GebSKI V, et al. EUS-FNA biopsies to guide precision medicine in pancreatic cancer: results of a pilot study to identify KRAS wild-type tumours for targeted therapy. *Front Oncol.* 2021;11: 770022.